Testing the accuracy of the overlap criterion

M. Mestre*, P.M. Cincotta, C.M. Giordano

Facultad de Ciencias Astronómicas y Geofísicas, Universidad Nacional de La Plata and Instituto de Astrofísica de La Plata (CONICET), Paseo del Bosque, B1900FWA La Plata, Argentina

ABSTRACT

Here we investigate the accuracy of the overlap criterion when applied to a simple near-integrable model in both its 2D and 3D versions. To this end, we consider, respectively, two and three quartic oscillators as the unperturbed system, and couple the degrees of freedom by a cubic, non-integrable perturbation. For both systems we compute the unperturbed resonances up to order $\mathcal{O}(\varepsilon^2)$, and model each resonance by means of the pendulum approximation in order to estimate the theoretical critical value of the perturbation parameter for a global transition to chaos. We perform several surface of sections for the bi-dimensional case to derive an empirical value to be compared to our theoretical estimation. Although both values are of the same order of magnitude, there is a significant difference between them. For the 3D case a numerical estimate is attained that we observe matches quite well the critical value resulting from theoretical means. This confirms once again that calculating resonances up to $\mathcal{O}(\varepsilon^2)$ suffices in order the overlap criterion to work out.

© 2008 Elsevier Ltd. All rights reserved.

1. Introduction

Though the stability problem of Hamiltonian systems has been almost completely elucidated by a rigorous sequence of theorems that build up the so called KAM theory (see for instance [1,2,6], together with the original references therein: [3–5]), the application of the results of the KAM theory to a specific system is far from being an easy task. In fact, it turns out to be much simpler to take advantage of the heuristic overlap criterion, which seems to provide similar estimations to those resulting from the KAM theory.

The overlap criterion due to Chirikov (see [1]) has been largely used in many different fields, its probably most popular application being the study of instabilities in the Solar System as well as in other planetary models (see for example [7–9]). In any case, since the widespread model for a resonance is the pendulum approximation, the overlap criterion applies directly to the intersection of their associated unperturbed separatrices (or heteroclinic intersections).

In his pioneer work on the standard map [1] Chirikov shows that the application of the overlap criterion to primary resonances overestimates the actual value of the critical parameter, K_c, and only when high order resonances are considered, does the overlap

criterion succeed in providing a more accurate value for K_c. In fact, the author shows that on including the third harmonic resonances, the overlap criterion leads to $K_c \approx 1$, rather close to the empirical value.

In the present effort we address a similar analysis to that performed by Chirikov, but using a 2D and a 3D near-integrable Hamiltonian systems, namely, two and three uncoupled quartic oscillators perturbed by a cubic term. The 3D version of this model has been studied in [10,12], where the authors numerically investigate the global dynamical properties of the model and estimate the critical value ε_c beyond which the system is globally chaotic, i.e. for which less than the 10% of the energy surface corresponds to invariant tori. By means of the overlap criterion we derive such a critical value for the perturbative parameter ε on considering not only primary but also high order resonances, and the perturbation Fourier series truncated at $\mathcal{O}(23^{-2})$ in their coefficients. We then compare, for each case, the theoretical critical value with that obtained by numerical means.

The paper is organized as follows. The dynamical system under study in its 2D version is described in Section 2 and its relevant resonances at $\mathcal{O}(\varepsilon)$ are obtained in Section 3, their widths being determined in Section 4. The resonances at $\mathcal{O}(\varepsilon^2)$ are provided in Section 5, where an estimate of the critical value of the perturbative parameter is provided. For the sake of comparison, an empirical estimate of such a value is obtained in Section 6 by recourse of performing several surfaces of section (SOS) for the system. The 3D model is addressed in Section 7, whose resonances at order $\mathcal{O}(\varepsilon)$ and $\mathcal{O}(\varepsilon^2)$ are given in Sections 8 and 9, respectively. Section 10 is devoted to the

* Corresponding author.

E-mail addresses: mmestre@fcaglp.unlp.edu.ar (M. Mestre), pmc@fcaglp.unlp.edu.ar (P.M. Cincotta), giordano@fcaglp.unlp.edu.ar (C.M. Giordano).

theoretical estimate of the critical parameter, which is shown to be in good agreement with the one given in [12]. A final discussion is provided in Section 11.

2. The 2D dynamical system

Here we will be concerned first with a 2D perturbed quartic oscillator. In cartesian coordinates the system is described by the following Hamiltonian (see [10]):

$$\tilde{H}(\boldsymbol{p},\boldsymbol{q}) = \tfrac{1}{2}(p_x^2 + p_y^2) + \tfrac{1}{4}(x^4 + y^4) + \varepsilon x^2 y, \tag{1}$$

where ε is a perturbative parameter that controls the strength of the perturbation. On setting $\varepsilon = 0$ we recover the integrable quartic oscillator's Hamiltonian (see [10,11] and references therein), whose solutions are given by

$$x(t) = x_0(h_1) \sum_{n=1}^{\infty} \alpha_n \cos((2n-1)\omega_1(h_1)t),$$

$$y(t) = y_0(h_2) \sum_{n=1}^{\infty} \alpha_n \cos((2n-1)\omega_2(h_2)t), \tag{2}$$

where we have used the following definitions:

$$x_0(h_1) = 4\beta h_1^{1/4},$$

$$y_0(h_2) = 4\beta h_2^{1/4},$$

$$\omega_i(h_i) = \sqrt{2}\beta h_i^{1/4}, \quad i = 1, 2$$

$$\alpha_n = \frac{1}{\cosh((n-1/2)\pi)},$$

$$\beta = \pi/2K(1/\sqrt{2}) \approx 0.847, \tag{3}$$

where $K(k)$ denotes the complete elliptic integral, and the coefficients in the Fourier expansions (2) satisfy

$$\frac{\alpha_{n+1}}{\alpha_n} \approx \frac{1}{23}.$$

The third equation in (3) reveals the dependence of the frequencies on the unperturbed energies, enabling us to get the functional relationship between the latter and the unperturbed action variables, namely, $h_i = A I_i^{4/3}$, with $A = (3\beta/2\sqrt{2})^{4/3}$.

With this relation in mind, and taking into account that the angle variables are $\theta_i \equiv \omega_i(h_i)t, i = 1, 2$, the complete Hamiltonian, in terms of the action-angle variables of the unperturbed Hamiltonian, can be recast as

$$H(\boldsymbol{I}, \boldsymbol{\theta}) = H_0(\boldsymbol{I}) + \varepsilon V(\boldsymbol{I}, \boldsymbol{\theta}), \tag{4}$$

where

$$H_0(\boldsymbol{I}) = A(I_1^{4/3} + I_2^{4/3}),$$

$$V(\boldsymbol{I}, \boldsymbol{\theta}) = \hat{V}(\boldsymbol{I}) \sum_{n,m,k=1}^{\infty} \alpha_{nmk}\{\cos(2(n+m-1)\theta_1 \pm (2k-1)\theta_2)$$

$$+ \cos(2(n-m)\theta_1 \pm (2k-1)\theta_2)\} \tag{5}$$

with $\alpha_{nmk} \equiv \alpha_n\alpha_m\alpha_k$, and $\hat{V}(\boldsymbol{I}) \equiv 2^{5/2}3\beta^4 I_1^{2/3} I_2^{1/3}$, the $\pm$ sign meaning that both terms are included in the series.

3. Resonances at $\mathcal{O}(\epsilon)$

A glance at the perturbation series given in Eq. (5) reveals that the number of resonant terms at first order in the perturbative parameter

Table 1
Harmonics in the Fourier expansion (5) at $\mathcal{O}(\varepsilon, 1/23^2)$

Vector	N_0	N_1	N_2	Vector	N_0	N_1	N_2
(2,1)	1	1	0	(2,−1)	1	1	0
(0,1)	1	0	1	(0,−1)	1	0	1
(2,3)	0	1	1	(2,−3)	0	1	1
(0,3)	0	1	0	(0,−3)	0	1	0
(2,5)	0	0	1	(2,−5)	0	0	1
(0,5)	0	0	1	(0,−5)	0	0	1
(4,1)	0	2	1	(4,−1)	0	2	1
(−2,1)	0	1	0	(−2,−1)	0	1	0
(4,3)	0	0	2	(4,−3)	0	0	2
(−2,3)	0	0	1	(−2,−3)	0	0	1
(6,1)	0	0	3	(6,−1)	0	0	3
(−4,1)	0	0	1	(−4,−1)	0	0	1

is unbounded, which is a drawback to take into account the width of every resonance at such an order.

However, the strong dependence of the Fourier amplitudes on $(n+m+k)$, through the quantities $\alpha_{nmk} \approx 1/23^{(n+m+k-3)}$, gives us a good hint on how to gather the $\mathcal{O}(\varepsilon)$ resonances and where to cut the series, our attempt being to keep terms only up to $\mathcal{O}(1/23^2)$.

All the possible combinations of n, m and k verifying that $n+m+k \leqslant 5$, yield 24 different vectors which are listed in Table 1, together with the number of times they appear in a term with coefficient α_{nmk} of a given order in $\frac{1}{23}$. Thus, N_0 denotes the number of times the vector appears with coefficient $\alpha_{nmk} = \alpha_1^3$, N_1 the number of times it arises with coefficient $\alpha_1^2\alpha_2(\approx \alpha_1^3/23)$, and N_2 corresponds to either the coefficient $\alpha_1\alpha_2^2$ or $\alpha_1^2\alpha_3$ (which are approximately $\alpha_1^3/23^2$). From now on, these vectors will be appointed as harmonics at order $\mathcal{O}(\varepsilon, 1/23^2)$.

On applying the resonance condition $\boldsymbol{m}\cdot\boldsymbol{\omega} = 0$, with $\boldsymbol{m} \in \mathbb{Z}^2/\{\boldsymbol{0}\}$, to the unperturbed system, the following relation between the energies in each degree of freedom is obtained:

$$m_1 h_1^{1/4} + m_2 h_2^{1/4} = 0, \tag{6}$$

which implies that the resonance structure in energy and action space consists of straight lines (with positive slope) given by

$$h_2^r = \frac{m_1^4}{m_2^4} h_1^r \tag{7}$$

and

$$I_2^r = \left|\frac{m_1^3}{m_2^3}\right| I_1^r, \tag{8}$$

respectively.

Moreover, Eq. (6) indicates that $m_1 m_2 \leqslant 0$, whence, those vectors having both components with the same sign must be discarded. Let us notice, however, that not all of the remaining harmonics at order $\mathcal{O}(\varepsilon, 1/23^2)$ are actually resonant, as it will be discussed in the forthcoming section.

4. Width of the resonances at $\mathcal{O}(\epsilon)$

On computing the width of resonances, the pendulum's approximation (see for instance [1,13]) provides a suitable description whenever each resonance is assumed to be isolated from the rest.

It should be noted that, before proceeding to estimate the width of a given resonance, all the coefficients α_{nmk} associated with the same trigonometric function are to be added together into a single one. Indeed, for each given vector $\boldsymbol{m}$, we should define the coefficient:

$$\alpha_{\boldsymbol{m}} \equiv \sum_{m+n+k \leqslant 5} \alpha_{nmk},$$

where n, m and k are natural numbers that combine to form the vector $\boldsymbol{m}$ in any of the four ways displayed in Eq. (5). Let us remark that $\alpha_{\boldsymbol{m}} \approx \alpha_1^3(N_0 + N_1/23 + N_2/23^2)$.

Inasmuch the pendulum's approximation has been applied to this single resonant term, the new (resonant) Hamiltonian turns out to be

$$H_r(p_1, \psi_1) = \frac{p_1^2}{2M} + \varepsilon \hat{V}(\boldsymbol{I^r}) \alpha_{\boldsymbol{m}} \cos \psi_1 \tag{9}$$

with

$$M^{-1} \equiv m_i \frac{\partial \omega_i^r}{\partial I_j} m_j = m_i^2 \frac{\partial \omega_i^r}{\partial I_i}, \quad \boldsymbol{I} = \boldsymbol{I^r} + \boldsymbol{m} p_1, \quad \psi_1 = \boldsymbol{m} \cdot \boldsymbol{\theta}, \tag{10}$$

where the sum over repeated indexes should be understood.

Let p_r be the maximum variation of p_1 within the oscillation regime, then

$$p_r = 2(\varepsilon M \hat{V}(\boldsymbol{I^r}) \alpha_{nmk})^{1/2} = 2^{7/2} \beta^{1/2} \left| \frac{m_1^3 m_2^{-1}}{m_1^4 + m_2^4} \right|^{1/2} \varepsilon^{1/2} \alpha_{nmk}^{1/2} (h_1^r)^{5/8}. \tag{11}$$

As a consequence of the simple pendulum dynamics, the maximum displacement of the unperturbed action variables depends on $\boldsymbol{m}$ and p_r in the fashion: $(\Delta \boldsymbol{I})^{\boldsymbol{r}} \equiv (\boldsymbol{I} - \boldsymbol{I^r})_{max} = p_r \boldsymbol{m}$.

Furthermore, the maximum displacement of the unperturbed energy is given by $|(\Delta h_i)_{\boldsymbol{m}}^r| = |\omega_i^r (\Delta l_i)_{\boldsymbol{m}}^r|$; and it is the maximum amplitude attained in the oscillation of any of the unperturbed energies that measures the width of the resonance.

Let us now recall that in any 2D problem the energy conservation condition $h = h_1 + h_2$, together with the resonance condition $m_1 h_1^{1/4} + m_2 h_2^{1/4} = 0$ allow both h_1^r and h_2^r to be written in terms of the total unperturbed energy h. Thus, the amplitude can be recast in terms of m_1, m_2, ε, $\alpha_{\boldsymbol{m}}$ and h as follows:

$$|(\Delta h_1)_{\boldsymbol{m}}^r| = 2^4 \beta^{3/2} \frac{|m_1|^{5/2} |m_2|^3}{|m_1^4 + m_2^4|^{11/8}} \varepsilon^{1/2} \alpha_{\boldsymbol{m}}^{1/2} h^{r7/8},$$

$$|(\Delta h_2)_{\boldsymbol{m}}^r| = |(\Delta h_1)_{\boldsymbol{m}}^r|. \tag{12}$$

The last identity in (12) is due to the fact that in presence of a single resonance, the motion of the system is tangent to the unperturbed energy surface, and for this particular model such a surface is given by $h = h_1 + h_2$, which leads to $\Delta h_2 = -\Delta h_1$.

We note that the width of the resonances at $\mathcal{O}(\varepsilon, 1/23^2)$ depends on the harmonic numbers in the manner shown in Fig. 1, so that those resonances with values of $\gamma = m_2/m_1$ out of the range $[0.5, 2.5]$ should be narrow.

A glance at both Eq. (12) and Fig. 1 reveals that those harmonic vectors with any of its components equal to zero do not change the energies, and consequently, they should not be considered as resonant vectors.

Further, since the perturbation terms are even, if $\boldsymbol{m}$ is a resonant vector then $-\boldsymbol{m}$ is also a resonant one (both corresponding to the same resonance). Hence, for each resonance just one representative resonant vector can be considered, encompassing into its concomitant coefficient the contribution corresponding to its opposite vector as well. All the relevant data required to compute the width of each resonance at $\mathcal{O}(\varepsilon, 1/23^2)$ are displayed in Table 2, where we have also included the value of h_1^r corresponding to a total unperturbed energy of $h = 1/(4\beta^4) \approx 0.485$ (the one used in [10]).

We have computed the resonance widths corresponding to ε in the range $[0, 0.5]$. Fig. 2 displays both the maximum and minimum values of h_1 for each resonance vs. the perturbative parameter ε; the total unperturbed energy being $h = 1/(4\beta^4)$. We observe that for $\varepsilon \sim 0.15$, the $(6, -1), (4, -1), (2-1)$ and $(4, -3)$ resonances do overlap,
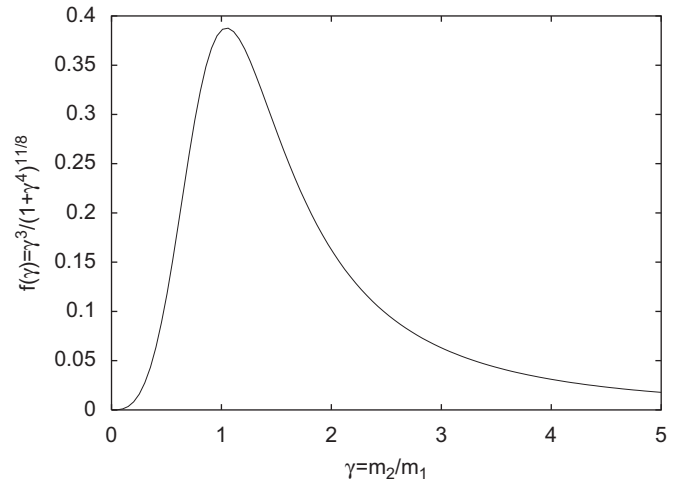

Fig. 1. Dependence of the resonance width on m_2/m_1.

Table 2
Resonant vectors at $\mathcal{O}(\varepsilon)$ up to $\mathcal{O}(1/23^2)$

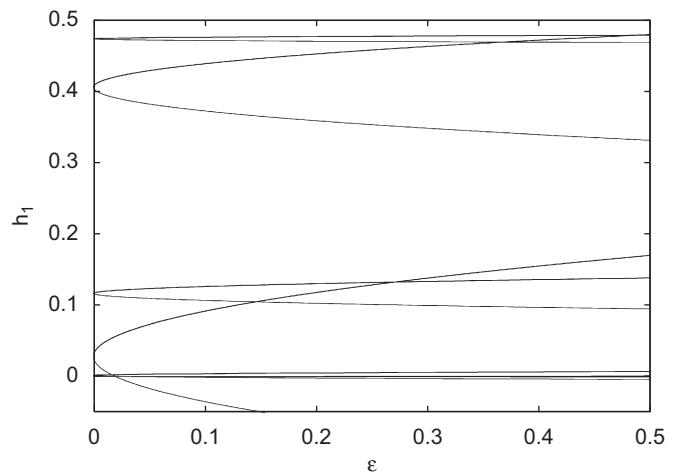| Vector	N_0	N_1	N_2	h_1^r
$(2, -5)$	0	0	1	0.4729
$(2, -3)$	0	1	2	0.4050
$(4, -3)$	0	0	2	0.1166
$(2, -1)$	1	2	0	0.0285
$(4, -1)$	0	2	2	0.0019
$(6, -1)$	0	0	3	0.0004

Fig. 2. Widths of those resonances at $\mathcal{O}(\varepsilon)$ up to $\mathcal{O}(1/23^2)$, in terms of ε.

but lie far away from the $(2, -3)$ and $(2, -5)$ resonances. Therefrom we could infer that the energy surface presents two unconnected regions of chaotic motion, so that a global transition to chaos does not take place for $\varepsilon \lesssim 0.5$, which leads to a critical theoretical value for the perturbation parameter $\varepsilon_c \gtrsim 0.5$.

5. Resonances at $\mathcal{O}(\epsilon^2)$

In those regions of phase space which are far from any primary resonance (i.e. where the diophantic condition holds for every primary resonance), we can introduce new cononical variables, $(\boldsymbol{J}, \boldsymbol{\varphi})$, in such a fashion that the transformed Hamiltonian consists of a part depending on the new momentum and a perturbation that, though

being non-integrable, has an amplitude of $\mathcal{O}(\varepsilon^2)$.

$$\mathscr{H}(\boldsymbol{J},\boldsymbol{\varphi})=H_0(\boldsymbol{J})+\varepsilon^2\left\{\frac{1}{2}\frac{\partial^2 H_0(\boldsymbol{J})}{\partial J_j\partial J_i}\frac{\partial\Phi(\boldsymbol{J},\boldsymbol{\varphi})}{\partial\varphi_j}\frac{\partial\Phi(\boldsymbol{J},\boldsymbol{\varphi})}{\partial\varphi_i}+\frac{\partial V(\boldsymbol{J},\boldsymbol{\varphi})}{\partial J_i}\frac{\partial\Phi(\boldsymbol{J},\boldsymbol{\varphi})}{\partial\varphi_i}\right\}$$
$$+\mathcal{O}(\varepsilon^3),\qquad(13)$$

where Φ stands for the trigonometric part of the generatrix function of the canonical transformation:

$$F(\boldsymbol{J},\boldsymbol{\theta})=\boldsymbol{J}\cdot\boldsymbol{\theta}+\varepsilon\Phi(\boldsymbol{J},\boldsymbol{\theta})\quad\Phi(\boldsymbol{J},\boldsymbol{\theta})=\sum_{\boldsymbol{m}\in\mathbb{Z}^2/\{\boldsymbol{0}\}}\Phi_{\boldsymbol{m}}(\boldsymbol{J})\sin(\boldsymbol{m}\cdot\boldsymbol{\theta})$$

with $\Phi_{\boldsymbol{m}}(\boldsymbol{J})=-V_{\boldsymbol{m}}(\boldsymbol{J})/\boldsymbol{m}\cdot\boldsymbol{\omega}(\boldsymbol{J})$.

After computing the right side of expression (13) one finds

$$\mathscr{H}(\boldsymbol{J},\boldsymbol{\varphi})=H_0(\boldsymbol{J})+\varepsilon^2\sum_{\boldsymbol{m},\boldsymbol{m}'}\mathbb{C}(\boldsymbol{m},\boldsymbol{m}',\boldsymbol{J})$$
$$\times\{\cos((\boldsymbol{m}+\boldsymbol{m}')\cdot\boldsymbol{\varphi})+\cos((\boldsymbol{m}-\boldsymbol{m}')\cdot\boldsymbol{\varphi})\}+\mathcal{O}(\varepsilon^3),\qquad(14)$$

where the coefficients are given by

$$\mathbb{C}(\boldsymbol{m},\boldsymbol{m}',\boldsymbol{J})=\alpha_{\boldsymbol{m}}\alpha_{\boldsymbol{m}'}\left\{2^3 3^{4/3}\beta^{28/3}\frac{(m_1 m_1' J_1^{2/3}J_2^{2/3}+m_2 m_2' J_1^{4/3})}{(\boldsymbol{m}\cdot\boldsymbol{\omega}(\boldsymbol{J}))(\boldsymbol{m}'\cdot\boldsymbol{\omega}(\boldsymbol{J}))}\right.$$
$$\left.-2^4 3\beta^8\frac{(2m_1' J_1^{1/3}J_2^{2/3}+m_2' J_1^{4/3}J_2^{-1/3})}{(\boldsymbol{m}'\cdot\boldsymbol{\omega}(\boldsymbol{J}))}\right\}.$$

There are several relevant facts to be remarked: (i) On working at $\mathcal{O}(\varepsilon)$ we have only considered resonances up to $\mathcal{O}(1/23^2)$ in the Fourier coefficients; therefore, the series in Eq. (14) should actually be replaced by a finite sum over those harmonics, $\boldsymbol{m}$ and $\boldsymbol{m}'$, whose associated coefficients ($\alpha_{\boldsymbol{m}}$ and $\alpha_{\boldsymbol{m}'}$, respectively) are such that their product is of order either α_1^6, $\alpha_1^6/23$ or $\alpha_1^6/23^2$. (ii) There are many different pairs of harmonics $(\boldsymbol{m},\boldsymbol{m}')$ at $\mathcal{O}(\varepsilon)$, which combine into the same harmonic $\boldsymbol{n}$ at $\mathcal{O}(\varepsilon^2)$. (iii) As a consequence of the evenness of the perturbation term, if $\boldsymbol{n}$ is a resonant vector $-\boldsymbol{n}$ is also a resonant one. (iv) The resonance condition implies that $n_1 n_2\leqslant 0$. (v) The condition of being far from resonances at $\mathcal{O}(\varepsilon)$ implies that we must discard all those harmonics which are a multiple of any resonant vector at $\mathcal{O}(\varepsilon,1/23^2)$.

To cope with the situation set up by the issues (ii) and (iii), we have added all the concomitant contributions into a single coefficient $\mathbb{D}$, namely,

$$\mathbb{D}(\boldsymbol{n},\boldsymbol{J})=\sum_{\boldsymbol{m},\boldsymbol{m}'}\mathbb{C}(\boldsymbol{m},\boldsymbol{m}',\boldsymbol{J}),\qquad(15)$$

where the sum extents to all the harmonics $(\boldsymbol{m},\boldsymbol{m}')$ at $\mathcal{O}(\varepsilon,1/23^2)$ such that $\boldsymbol{n}=\boldsymbol{m}+\boldsymbol{m}'$, $\boldsymbol{n}=\boldsymbol{m}-\boldsymbol{m}'$, $-\boldsymbol{n}=\boldsymbol{m}+\boldsymbol{m}'$, or $-\boldsymbol{n}=\boldsymbol{m}-\boldsymbol{m}'$, and for which $\mathcal{O}(\alpha_{\boldsymbol{m}}\alpha_{\boldsymbol{m}'})$ is not greater than $\alpha_1^6/23^2$.

Taking into account all the above mentioned considerations, the Hamiltonian can be written in the form:

$$\mathscr{H}(\boldsymbol{J},\boldsymbol{\varphi})=H_0(\boldsymbol{J})+\varepsilon^2\sum_{\boldsymbol{n}}\mathbb{D}(\boldsymbol{n},\boldsymbol{J})\cos(\boldsymbol{n}\cdot\boldsymbol{\varphi}).\qquad(16)$$

Therefore, in the vicinity of a resonant torus $\boldsymbol{J}^r$, and by recourse of the pendulum approximation, we obtain the new resonant Hamiltonian:

$$\mathscr{H}_r(\mathscr{P}_1,\Psi_1)=\frac{\mathscr{P}_1^2}{2\mu}+\mathscr{U}_0\cos(\Psi_1),\qquad(17)$$

Table 3
Resonant vectors of $\mathcal{O}(\varepsilon^2)$ up to $\mathcal{O}(1/23^2)$

Vector	h_1^r
$(2,-6)$	0.4791
$(2,-4)$	0.4565
$(2,-2)$	0.2425
$(6,-4)$	0.0800
$(6,-2)$	0.0059
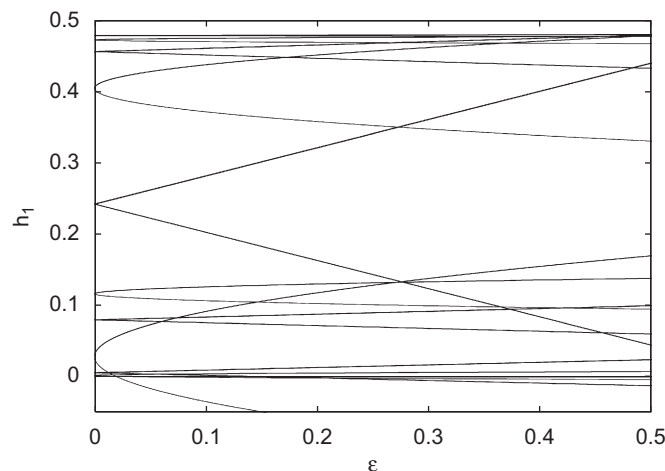
Fig. 3. Width of the resonances up to $\mathcal{O}(\varepsilon^2,1/23^2)$ vs. ε.

where

$$\mu^{-1}\equiv n_i\frac{\partial\omega_i^r}{\partial J_j}n_j,$$
$$\mathscr{U}_0\equiv\varepsilon^2\mathbb{D}(\boldsymbol{n},\boldsymbol{J}^{\boldsymbol{r}}).\qquad(18)$$

Thus, the maximum displacement of the unperturbed action variables is given by $(\Delta\boldsymbol{J})^{\boldsymbol{r}}\equiv(\boldsymbol{J}-\boldsymbol{J}^{\boldsymbol{r}})_{max}=\mathscr{P}_r\boldsymbol{n}$, with $\mathscr{P}_r=2(\mu|\mathscr{U}_0|)^{1/2}$, and the widths of the resonances at $\mathcal{O}(\varepsilon^2)$ are given by

$$|(\Delta h_1)_{\boldsymbol{n}}^r|=2^4\beta^3 h^{3/4}\varepsilon\frac{|n_2|^3 n_1^2}{(n_1^4+n_2^4)^{5/4}}\cdot\left|\sum_{\boldsymbol{m},\boldsymbol{m}'}\alpha_{\boldsymbol{m}}\alpha_{\boldsymbol{m}'}\right.$$
$$\left.\left\{\frac{2(2|n_1|^3 m_1'+|n_2|^3 m_2')}{|n_1 n_2|(m_1'|n_2|+m_2'|n_1|)}\pm\frac{n_1^2 m_1' m_1+n_2^2 m_2' m_2}{(m_1'|n_2|+m_2'|n_1|)^2}\right\}\right|^{1/2},$$

where the plus sign corresponds to $\boldsymbol{n}=\boldsymbol{m}+\boldsymbol{m}'$ and the minus sign to $\boldsymbol{n}=\boldsymbol{m}-\boldsymbol{m}'$, m_i ought to be written in terms of m_i' and n_i. As a consequence of this last expression, resonant vectors are compelled to have no null components.

The harmonics satisfying all the stated conditions for the perturbation at order ε^2 turn out to be just five, which are listed in Table 3. They will be referred to as resonant vectors at $\mathcal{O}(\varepsilon^2,1/23^2)$. We have computed the concomitant resonance widths for ε in the range $[0,0.5]$. The results are presented in Fig. 3, where also the resonances corresponding to $\mathcal{O}(\varepsilon)$ have been included. Let us recall that the adopted value for the total unperturbed energy is $h=1/4\beta^4$.

From Fig. 3 and Table 3 we notice that the arising of the $(2,-2)$ resonance connects the two sets of resonances that at $\mathcal{O}(\varepsilon,1/23^2)$ appeared isolated for the considered ε range. The remaining resonances at $\mathcal{O}(\varepsilon^2,1/23^2)$ appear completely overlapped with either set of resonances at $\mathcal{O}(\varepsilon,1/23^2)$. From this plot, we could derive the critical value for the perturbative parameter, $\varepsilon_c\approx 0.28$.
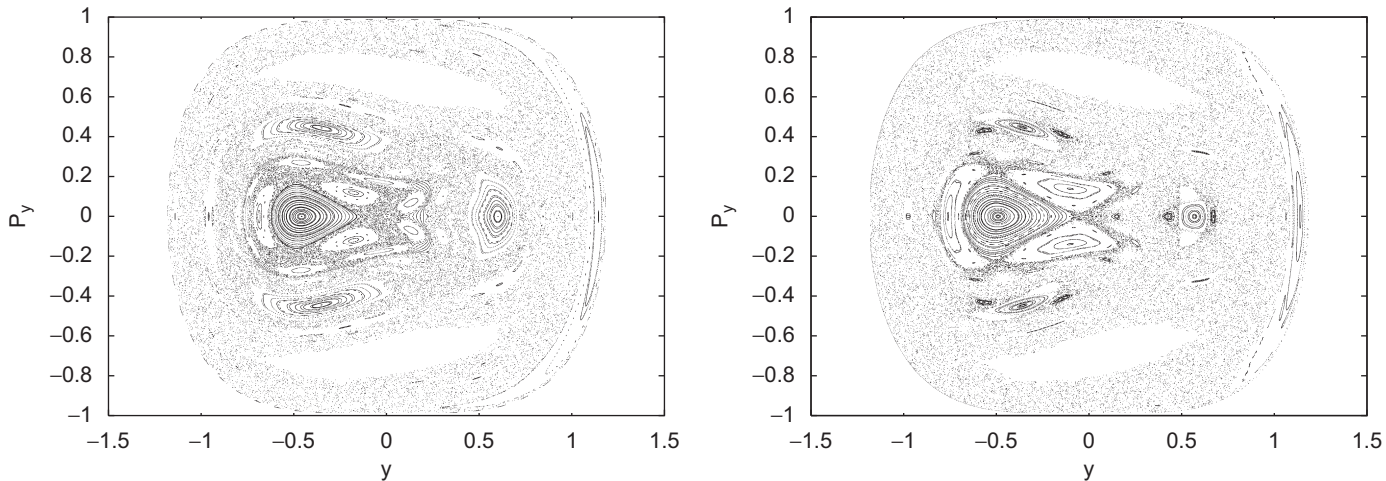
Fig. 4. Poincaré surfaces of section for $\varepsilon = 0.12$ (on the left), and for $\varepsilon = 0.14$ (on the right).

6. Numerical estimation of the critical value of the perturbation parameter

In this section we empirically estimate the value of ε_c by means of Poincaré SOS. To this aim, we take the intersections on the plane $x=0$ (actually $|x| < 10^{-8}$) whenever $p_x > 0$, for several initial conditions along the y-axis.

Fig. 4 displays the SOSs corresponding to $\varepsilon = 0.12$ (on the left) and 0.14 (on the right), respectively. There we can distinguish the $(2, -1)$ resonance, very close to the last invariant curve that corresponds to the y-axis periodic orbit—$(1, 0)$ resonance—and the $(2, -2), (2, -3)$ resonances as well. The $(2, -4)$, $(2, -5)$ and $(2, -6)$ resonances do not show up due to the fact that they are completely destroyed by overlap, as could be seen from Fig. 3 for this value of ε. It is important to remark that several higher order resonances do appear which have not been theoretically computed.

For $\varepsilon = 0.12$, we observe that the chaotic domain where the $(2, -4)$, $(2, -5)$ and $(2, -6)$ resonances appear destroyed by overlap is bounded by some KAM tori and thus, it remains unconnected with the outer chaotic component around the $(2, -3)$ and $(2, -1)$ resonances. On the other hand, for $\varepsilon = 0.14$, both chaotic zones are connected, leading to a global transition to chaos, in the sense that any orbit could explore almost all the chaotic component of phase space.

Therefore, it looks like ε_c lies somewhere in the range $(0.12, 0.14)$. After performing a rather thorough numerical exploration, we have noted that for $\varepsilon = 0.135$, several KAM tori do persist, which are shown in Fig. 5, where a zoom in the window $[0, 0.4] \times [0, 0.3]$ is presented. There, such KAM tori can be clearly distinguished and are seen to definitively separate both chaotic domains in phase space. Nevertheless, this bounded region of chaotic motion, does not involve the resonances we are taking into account to derive the analytical estimation of ε_c, but high order ones.

Therefore, from experimental means, we may state that $\varepsilon \gtrsim 0.135$ is a good lower bound for the critical value of the perturbation parameter.

7. The 3D model

Now we will focus on a 3D version of the dynamical system under study. In Cartesian coordinates, its Hamiltonian is given by

$$\tilde{H}(\boldsymbol{p}, \boldsymbol{q}) = \tfrac{1}{2}(p_x^2 + p_y^2 + p_z^2) + \tfrac{1}{4}(x^4 + y^4 + z^4) + \varepsilon x^2(y + z). \quad (19)$$

Let us notice that for a null value of the perturbative parameter we recover the three independent 1D quartic oscillators, whose
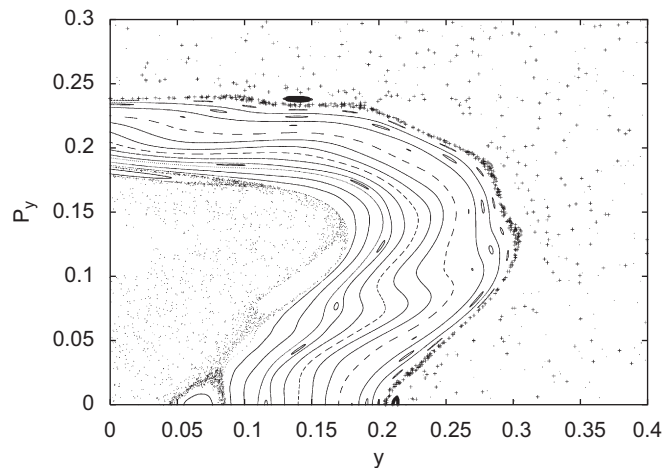

Fig. 5. Poincaré surface of section for $\varepsilon = 0.135$ illustrating the existence of KAM tori that separate both chaotic components.

solutions $x(t)$ and $y(t)$ are the ones given by Eq. (2), while $z(t)$ allows for the expression:

$$z(t) = z_0(h_3) \sum_{n=1}^{\infty} \alpha_n \cos((2n - 1)\omega_3(h_3)t), \quad (20)$$

where $z_0(h_3) = 4\beta h_3^{1/4}$.

In terms of the action-angle variables of the unperturbed Hamiltonian, the complete Hamiltonian (19) can be recast as

$$H(\boldsymbol{I}, \boldsymbol{\theta}) = H_0(\boldsymbol{I}) + \varepsilon V(\boldsymbol{I}, \boldsymbol{\theta}) \quad (21)$$

with

$$H_0(\boldsymbol{I}) = A(I_1^{4/3} + I_2^{4/3} + I_3^{4/3}),$$

$$\begin{aligned} V(\boldsymbol{I}, \boldsymbol{\theta}) = \hat{V}_{12}(\boldsymbol{I}) \sum_{n,m,k=1}^{\infty} \alpha_{nmk}\{&\cos(2(n+m-1)\theta_1 \pm (2k-1)\theta_2) \\ &+ \cos(2(n-m)\theta_1 \pm (2k-1)\theta_2)\} \\ + \hat{V}_{13}(\boldsymbol{I}) \sum_{n,m,k=1}^{\infty} \alpha_{nmk}\{&\cos 2(n+m-1)\theta_1 \pm (2k-1)\theta_3) \\ &+ \cos(2(n-m)\theta_1 \pm (2k-1)\theta_3)\}, \quad (22) \end{aligned}$$

where the new quantities $\hat{V}_{1j}(\mathbf{I}) \equiv 2^{5/2}3\beta^4 I_1^{2/3}I_j^{1/3}$ have been introduced; the $\pm$ sign meaning that both terms are included in the series.

8. Resonances at $\mathcal{O}(\epsilon)$

The perturbation given in Eq. (22) shows that for each combination of n, m and k there result 8 harmonic vectors $\mathbf{m}$. Again, due to the even character of the perturbation, we take just one representative resonant vector, $\mathbf{m}$, whose coefficient $\alpha_{\mathbf{m}}$ also encompasses the contribution of its opposite vector $-\mathbf{m}$; and keep only those harmonics such that $\mathcal{O}(\alpha_{\mathbf{m}}) \leqslant \mathcal{O}(1/23^2)$.

Since the harmonic vectors at $\mathcal{O}(\varepsilon, 1/23^2)$ can be splitted into two groups, we denote by $\mathcal{Y}$ the subset of vectors whose third component is zero and by $\mathcal{Z}$ that of vectors having their second component equal to zero. Therefore, the perturbation can be written in the fashion:

$$V(\mathbf{I}, \boldsymbol{\theta}) = \hat{V}_{12}(\mathbf{I}) \sum_{\mathbf{m}\in\mathcal{Y}} \alpha_{\mathbf{m}} \cos(\mathbf{m}\cdot\boldsymbol{\theta}) + \hat{V}_{13}(\mathbf{I}) \sum_{\mathbf{m}\in\mathcal{Z}} \alpha_{\mathbf{m}} \cos(\mathbf{m}\cdot\boldsymbol{\theta}). \quad (23)$$

On applying the resonance condition, $\mathbf{m}\cdot\boldsymbol{\omega}=0$, with $\mathbf{m} \in \mathbb{Z}^3/\{\mathbf{0}\}$, to the unperturbed system, the following relation between the actions in each degree of freedom is obtained:

$$m_1 I_1^{1/3} + m_2 I_2^{1/3} + m_3 I_3^{1/3} = 0 \quad (24)$$

so that each resonant vector could not have all its three components of the same sign. Furthermore, whenever a resonant vector has two of its components equal to zero, we get a null amplitude for the perturbation term.

Thus, we obtain 12 different resonant vectors, grouped in the following set:

$$\begin{aligned}\mathcal{V}_r(\varepsilon, 1/23^2) = \{&(2,-1,0),(2,-3,0),(2,-5,0),(4,-1,0),(4,-3,0),\\ &(6,-1,0),(2,0,-1),(2,0,-3),(2,0,-5),\\ &(4,0,-1),(4,0,-3),(6,0,-1)\}.\end{aligned}$$

For those vectors $\mathbf{m} \in \mathcal{Y}$, the resonance condition together with the energy conservation condition define a curve in action space (not just a point as in the 2D case) given by

$$\begin{cases} I_2^r = -\left(\dfrac{m_1}{m_2}\right)^3 I_1^r, \\ I_3^r = \left\{\dfrac{h}{A} - \left(1 + \dfrac{m_1^4}{m_2^4}\right)(I_1^r)^{4/3}\right\}^{3/4}, \end{cases} \quad (25)$$

where $I_1^r \in [0, I_{max}^{\mathcal{Y}}]$ with $I_{max}^{\mathcal{Y}} = (h/A/(1 + (m_1/m_2)^4))^{3/4}$.

The concomitant curve for $\mathbf{m} \in \mathcal{Z}$ is given by

$$\begin{cases} I_2^r = \left\{\dfrac{h}{A} - \left(1 + \dfrac{m_1^4}{m_3^4}\right)(I_1^r)^{4/3}\right\}^{3/4}, \\ I_3^r = -\left(\dfrac{m_1}{m_3}\right)^3 I_1^r \end{cases} \quad (26)$$

with $I_1^r \in [0, I_{max}^{\mathcal{Z}}]$, the upper bound being $I_{max}^{\mathcal{Z}} = (h/A/(1 + (m_1/m_3)^4))^{3/4}$. In energy surface both kind of resonances define straight lines. On applying the pendulum approximation, we obtain a similar resonant Hamiltonian to that given by Eq. (9), namely,

$$H_r(p_1, \psi_1) = \frac{p_1^2}{2M} + \varepsilon V_{\mathbf{m}} \cos\psi_1, \quad (27)$$

where $V_{\mathbf{m}} = \hat{V}_{12}(\mathbf{I}^r)\alpha_{\mathbf{m}}$ for $\mathbf{m} \in \mathcal{Y}$ and $V_{\mathbf{m}} = \hat{V}_{13}(\mathbf{I}^r)\alpha_{\mathbf{m}}$ for $\mathbf{m} \in \mathcal{Z}$.

In energy space, the resonance widths in each degree of freedom, are adequately described by

$$\begin{aligned}(\Delta h_i)_{\mathbf{m}}^r = \omega_i(I_i^r)(\Delta I_i)_{\mathbf{m}}^r &= \tfrac{4}{3}A I_i^{1/3}2(\varepsilon M V_{\mathbf{m}})^{1/2}m_i \\ &= \tfrac{8}{3}A I_i^{1/3}(\varepsilon M V_{\mathbf{m}})^{1/2}m_i.\end{aligned} \quad (28)$$

Let us remark that, while in the 2D model the resonance and energy conservation conditions force the resonance width to depend on just one variable, either h, h_1^r or I_1^r, in the 3D model the resonance width is a function of two independent variables, which we have chosen to be I_1^r and h.

With the widths computed by means of (28), we can trace the displacements of the resonant energies, $h_i^r + (\Delta h_i)_{\mathbf{m}}^r$ and $h_i^r - (\Delta h_i)_{\mathbf{m}}^r$, for values of $I_1^r \in [0, I_{max}]$. Therefore, following [10] we perform the global change of coordinates:

$$e_1 = \tfrac{1}{\sqrt{6}}(h_1 - 2h_2 + h_3),$$

$$e_2 = \tfrac{1}{\sqrt{2}}(h_1 - h_3),$$

$$e_3 = \tfrac{1}{\sqrt{3}}(h_1 + h_2 + h_3), \quad (29)$$

where $e_1 \in [-(\sqrt{2/3})h, h/\sqrt{6}]$, $e_2 \in [-h/\sqrt{2}, h/\sqrt{2}]$ and $e_3 = h/\sqrt{3}$, adopting the value $h \approx 0.485$, to finally display in Fig. 6 the region of energy surface occupied by the structure of resonances at $\mathcal{O}(\varepsilon, 1/23^2)$ for two different values of the perturbative parameter. Let us remark that many of the resonances in $\mathcal{V}_r(\varepsilon, 1/23^2)$ are barely observable due to their thinness and close proximity to a boundary.
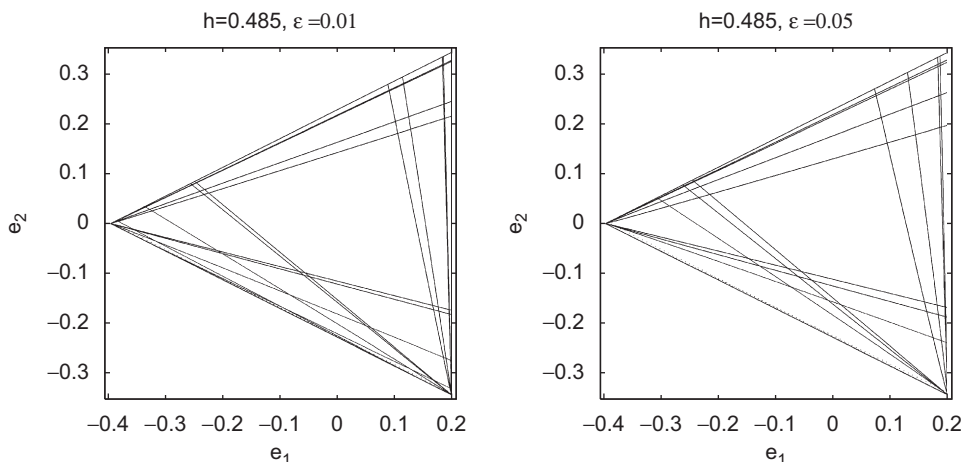

Fig. 6. Resonances at $\mathcal{O}(\varepsilon, 1/23^2)$ for $\varepsilon = 0.01$ (on the left) and $\varepsilon = 0.05$ (on the right).

9. Resonances at $\mathcal{O}(\epsilon^2)$

As in the 2D case, we perform a canonical transformation in order to remove the perturbation at $\mathcal{O}(\varepsilon)$, the associated generatrix function being of the form:

$$F(\boldsymbol{J},\boldsymbol{\theta}) = \boldsymbol{J}\cdot\boldsymbol{\theta} + \varepsilon\Phi(\boldsymbol{J},\boldsymbol{\theta}), \tag{30}$$

where

$$\Phi(\boldsymbol{J},\boldsymbol{\theta}) = \sum_{\boldsymbol{m}\in\mathscr{Y}} \Phi_{\boldsymbol{m}}(\boldsymbol{J})\sin(\boldsymbol{m}\cdot\boldsymbol{\theta}) + \sum_{\boldsymbol{m}\in\mathscr{Z}} \Phi_{\boldsymbol{m}}(\boldsymbol{J})\sin(\boldsymbol{m}\cdot\boldsymbol{\theta}) \tag{31}$$

with $\Phi_{\boldsymbol{m}}(\boldsymbol{J}) = -V_{\boldsymbol{m}}(\boldsymbol{J})/\boldsymbol{m}\cdot\omega(\boldsymbol{J})$.

The new Hamiltonian is described by the same formal expression given in Eq. (13), where the first and second terms within braces adopt the values:

$$\frac{1}{2}\frac{\partial^2 H_0(\boldsymbol{J})}{\partial J_j \partial J_i}\frac{\partial\Phi(\boldsymbol{J},\boldsymbol{\varphi})}{\partial\varphi_j}\frac{\partial\Phi(\boldsymbol{J},\boldsymbol{\varphi})}{\partial\varphi_i}$$

$$= \sum_{\boldsymbol{m}\in\mathscr{Y}}\sum_{\boldsymbol{m}'\in\mathscr{Y}} \delta_{\boldsymbol{m},\boldsymbol{m}'} \frac{(m_1 m_1' J_1^{2/3} J_2^{2/3} + m_2 m_2' J_1^{4/3})}{(m_1 J_1^{1/3} + m_2 J_2^{1/3})(m_1' J_1^{1/3} + m_2' J_2^{1/3})}$$
$$\times \{\cos((\boldsymbol{m}+\boldsymbol{m}')\cdot\boldsymbol{\varphi}) + \cos((\boldsymbol{m}-\boldsymbol{m}')\cdot\boldsymbol{\varphi})\}$$

$$+ \sum_{\boldsymbol{m}\in\mathscr{Z}}\sum_{\boldsymbol{m}'\in\mathscr{Z}} \delta_{\boldsymbol{m},\boldsymbol{m}'} \frac{(m_1 m_1' J_1^{2/3} J_3^{2/3} + m_3 m_3' J_1^{4/3})}{(m_1 J_1^{1/3} + m_3 J_3^{1/3})(m_1' J_1^{1/3} + m_3' J_3^{1/3})}$$
$$\times \{\cos((\boldsymbol{m}+\boldsymbol{m}')\cdot\boldsymbol{\varphi}) + \cos((\boldsymbol{m}-\boldsymbol{m}')\cdot\boldsymbol{\varphi})\}$$

$$+ \sum_{\boldsymbol{m}\in\mathscr{Y}}\sum_{\boldsymbol{m}'\in\mathscr{Z}} \delta_{\boldsymbol{m},\boldsymbol{m}'} \frac{m_1 m_1' J_1^{2/3} J_2^{1/3} J_3^{1/3}}{(m_1 J_1^{1/3} + m_2 J_2^{1/3})(m_1' J_1^{1/3} + m_3' J_3^{1/3})}$$
$$\times \{\cos((\boldsymbol{m}+\boldsymbol{m}')\cdot\boldsymbol{\varphi}) + \cos((\boldsymbol{m}-\boldsymbol{m}')\cdot\boldsymbol{\varphi})\}$$

$$+ \sum_{\boldsymbol{m}\in\mathscr{Z}}\sum_{\boldsymbol{m}'\in\mathscr{Y}} \delta_{\boldsymbol{m},\boldsymbol{m}'} \frac{m_1 m_1' J_1^{2/3} J_2^{1/3} J_3^{1/3}}{(m_1 J_1^{1/3} + m_3 J_3^{1/3})(m_1' J_1^{1/3} + m_2' J_2^{1/3})}$$
$$\times \{\cos((\boldsymbol{m}+\boldsymbol{m}')\cdot\boldsymbol{\varphi}) + \cos((\boldsymbol{m}-\boldsymbol{m}')\cdot\boldsymbol{\varphi})\}, \tag{32}$$

where $\delta_{\boldsymbol{m},\boldsymbol{m}'} = 2^3 3^{2/3}\beta^{20/3}\alpha_{\boldsymbol{m}}\alpha_{\boldsymbol{m}'}$ and

$$\frac{\partial V(\boldsymbol{J},\boldsymbol{\varphi})}{\partial J_i}\frac{\partial\Phi(\boldsymbol{J},\boldsymbol{\varphi})}{\partial\varphi_i}$$

$$= -\sum_{\boldsymbol{m}\in\mathscr{Y}}\sum_{\boldsymbol{m}'\in\mathscr{Y}} 2\delta_{\boldsymbol{m},\boldsymbol{m}'} \frac{(2m_1' J_1^{1/3} J_2^{2/3} + m_2' J_1^{4/3} J_2^{-1/3})}{(m_1' J_1^{1/3} + m_2' J_2^{1/3})}$$
$$\times \{\cos((\boldsymbol{m}+\boldsymbol{m}')\cdot\boldsymbol{\varphi}) + \cos((\boldsymbol{m}-\boldsymbol{m}')\cdot\boldsymbol{\varphi})\}$$

$$- \sum_{\boldsymbol{m}\in\mathscr{Z}}\sum_{\boldsymbol{m}'\in\mathscr{Z}} 2\delta_{\boldsymbol{m},\boldsymbol{m}'} \frac{(2m_1' J_1^{1/3} J_3^{2/3} + m_3' J_1^{4/3} J_3^{-1/3})}{(m_1' J_1^{1/3} + m_3' J_3^{1/3})}$$
$$\times \{\cos((\boldsymbol{m}+\boldsymbol{m}')\cdot\boldsymbol{\varphi}) + \cos((\boldsymbol{m}-\boldsymbol{m}')\cdot\boldsymbol{\varphi})\}$$

$$- \sum_{\boldsymbol{m}\in\mathscr{Y}}\sum_{\boldsymbol{m}'\in\mathscr{Z}} 2^2\delta_{\boldsymbol{m},\boldsymbol{m}'} \frac{m_1' J_1^{1/3} J_2^{1/3} J_3^{1/3}}{(m_1' J_1^{1/3} + m_3' J_3^{1/3})}$$
$$\times \{\cos((\boldsymbol{m}+\boldsymbol{m}')\cdot\boldsymbol{\varphi}) + \cos((\boldsymbol{m}-\boldsymbol{m}')\cdot\boldsymbol{\varphi})\}$$

$$- \sum_{\boldsymbol{m}\in\mathscr{Z}}\sum_{\boldsymbol{m}'\in\mathscr{Y}} 2^2\delta_{\boldsymbol{m},\boldsymbol{m}'} \frac{m_1' J_1^{1/3} J_2^{1/3} J_3^{1/3}}{(m_1' J_1^{1/3} + m_2' J_2^{1/3})}$$
$$\times \{\cos((\boldsymbol{m}+\boldsymbol{m}')\cdot\boldsymbol{\varphi}) + \cos((\boldsymbol{m}-\boldsymbol{m}')\cdot\boldsymbol{\varphi})\}. \tag{33}$$

Therefore, the Hamiltonian may be recast as

$$\mathscr{H}(\boldsymbol{J},\boldsymbol{\varphi})$$

$$= H_0(\boldsymbol{J}) + \varepsilon^2\sum_{\boldsymbol{n}\in\mathscr{A}}\left\{ \sum_{\boldsymbol{m}\in\mathscr{Y}}\sum_{\boldsymbol{m}'\in\mathscr{Y}} [a(\boldsymbol{n},\boldsymbol{m},\boldsymbol{m}',\boldsymbol{J}) + a(\boldsymbol{n},\boldsymbol{m},-\boldsymbol{m}',\boldsymbol{J})]\cos(\boldsymbol{n}\cdot\boldsymbol{\varphi}) \right.$$

$$+ \sum_{\boldsymbol{m}\in\mathscr{Z}}\sum_{\boldsymbol{m}'\in\mathscr{Z}} [b(\boldsymbol{n},\boldsymbol{m},\boldsymbol{m}',\boldsymbol{J}) + b(\boldsymbol{n},\boldsymbol{m},-\boldsymbol{m}',\boldsymbol{J})]\cos(\boldsymbol{n}\cdot\boldsymbol{\varphi})$$

$$+ \sum_{\boldsymbol{m}\in\mathscr{Y}}\sum_{\boldsymbol{m}'\in\mathscr{Z}} [c(\boldsymbol{n},\boldsymbol{m},\boldsymbol{m}',\boldsymbol{J}) + c(\boldsymbol{n},\boldsymbol{m},-\boldsymbol{m}',\boldsymbol{J})]\cos(\boldsymbol{n}\cdot\boldsymbol{\varphi})$$

$$\left. + \sum_{\boldsymbol{m}\in\mathscr{Z}}\sum_{\boldsymbol{m}'\in\mathscr{Y}} [d(\boldsymbol{n},\boldsymbol{m},\boldsymbol{m}',\boldsymbol{J}) + d(\boldsymbol{n},\boldsymbol{m},-\boldsymbol{m}',\boldsymbol{J})]\cos(\boldsymbol{n}\cdot\boldsymbol{\varphi}) \right\}, \tag{34}$$

where $\mathscr{A}$ is the set of harmonic vectors arising through any combination of vectors from $\mathscr{Y}\cup\mathscr{Z}$ and whose first non-zero component is positive, and the coefficients a–d are defined as follows:

$$a(\boldsymbol{n},\boldsymbol{m},\boldsymbol{m}',\boldsymbol{J})$$

$$= \begin{cases} \delta_{\boldsymbol{m},\boldsymbol{m}'}\left[\dfrac{(m_1 m_1' J_1^{2/3} J_2^{2/3} + m_2 m_2' J_1^{4/3})}{(m_1 J_1^{1/3} + m_2 J_2^{1/3})(m_1' J_1^{1/3} + m_2' J_2^{1/3})} \right. \\[6pt] \qquad \left. -2\dfrac{(2m_1' J_1^{1/3} J_2^{2/3} + m_2' J_1^{4/3} J_2^{-1/3})}{(m_1' J_1^{1/3} + m_2' J_2^{1/3})} \right] & \text{if } \pm\boldsymbol{n} = \boldsymbol{m}+\boldsymbol{m}', \\[10pt] 0 & \text{if } \pm\boldsymbol{n}\neq\boldsymbol{m}+\boldsymbol{m}'. \end{cases}$$

$$b(\boldsymbol{n},\boldsymbol{m},\boldsymbol{m}',\boldsymbol{J})$$

$$= \begin{cases} \delta_{\boldsymbol{m},\boldsymbol{m}'}\left[\dfrac{(m_1 m_1' J_1^{2/3} J_3^{2/3} + m_3 m_3' J_1^{4/3})}{(m_1 J_1^{1/3} + m_3 J_3^{1/3})(m_1' J_1^{1/3} + m_3' J_3^{1/3})} \right. \\[6pt] \qquad \left. -2\dfrac{(2m_1' J_1^{1/3} J_3^{2/3} + m_3' J_1^{4/3} J_3^{-1/3})}{(m_1' J_1^{1/3} + m_3' J_3^{1/3})} \right] & \text{if } \pm\boldsymbol{n} = \boldsymbol{m}+\boldsymbol{m}', \\[10pt] 0 & \text{if } \pm\boldsymbol{n}\neq\boldsymbol{m}+\boldsymbol{m}'. \end{cases}$$

$$c(\boldsymbol{n},\boldsymbol{m},\boldsymbol{m}',\boldsymbol{J})$$

$$= \begin{cases} \delta_{\boldsymbol{m},\boldsymbol{m}'}\left[\dfrac{m_1 m_1' J_1^{2/3} J_2^{1/3} J_3^{1/3}}{(m_1 J_1^{1/3} + m_2 J_2^{1/3})(m_1' J_1^{1/3} + m_3' J_3^{1/3})} \right. \\[6pt] \qquad \left. -4\dfrac{m_1' J_1^{1/3} J_2^{1/3} J_3^{1/3}}{(m_1' J_1^{1/3} + m_3' J_3^{1/3})} \right] & \text{if } \pm\boldsymbol{n} = \boldsymbol{m}+\boldsymbol{m}', \\[10pt] 0 & \text{if } \pm\boldsymbol{n}\neq\boldsymbol{m}+\boldsymbol{m}'. \end{cases}$$

$$d(\boldsymbol{n},\boldsymbol{m},\boldsymbol{m}',\boldsymbol{J})$$

$$= \begin{cases} \delta_{\boldsymbol{m},\boldsymbol{m}'}\left[\dfrac{m_1 m_1' J_1^{2/3} J_2^{1/3} J_3^{1/3}}{(m_1 J_1^{1/3} + m_3 J_3^{1/3})(m_1' J_1^{1/3} + m_2' J_2^{1/3})} \right. \\[6pt] \qquad \left. -4\dfrac{m_1' J_1^{1/3} J_2^{1/3} J_3^{1/3}}{(m_1' J_1^{1/3} + m_2' J_2^{1/3})} \right] & \text{if } \pm\boldsymbol{n} = \boldsymbol{m}+\boldsymbol{m}', \\[10pt] 0 & \text{if } \pm\boldsymbol{n}\neq\boldsymbol{m}+\boldsymbol{m}'. \end{cases}$$
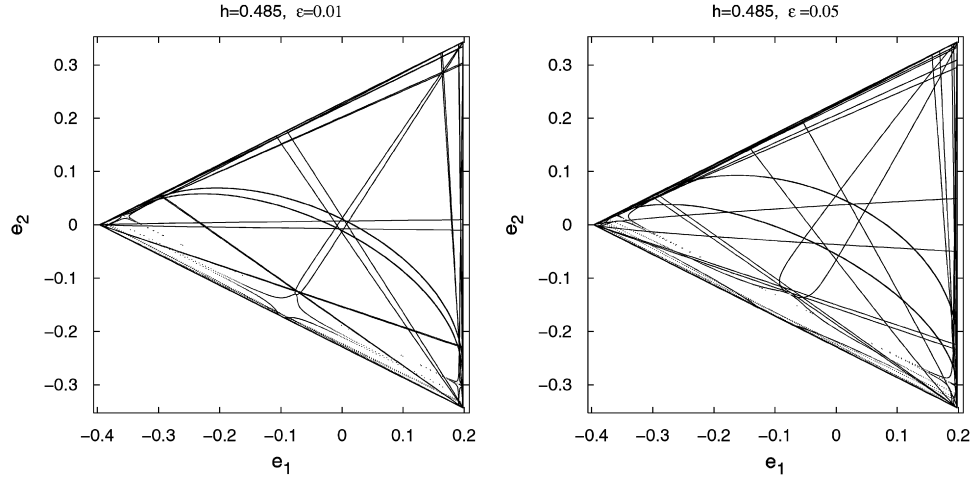
Fig. 7. Resonances at $\mathcal{O}(\varepsilon^2, 1/23^2)$ for $\varepsilon = 0.01$ (on the left) and $\varepsilon = 0.05$ (on the right).

Further, on introducing a coefficient analogous to the one in the perturbation at $\mathcal{O}(\varepsilon^2)$ for the 2D model,

$$\mathbb{D}(\boldsymbol{n},\boldsymbol{J}) = \sum_{\boldsymbol{m}\in\mathscr{Y}}\sum_{\boldsymbol{m}'\in\mathscr{Y}}[a(\boldsymbol{n},\boldsymbol{m},\boldsymbol{m}',\boldsymbol{J}) + a(\boldsymbol{n},\boldsymbol{m},-\boldsymbol{m}',\boldsymbol{J})]$$
$$+ \sum_{\boldsymbol{m}\in\mathscr{Z}}\sum_{\boldsymbol{m}'\in\mathscr{Z}}[b(\boldsymbol{n},\boldsymbol{m},\boldsymbol{m}',\boldsymbol{J}) + b(\boldsymbol{n},\boldsymbol{m},-\boldsymbol{m}',\boldsymbol{J})]$$
$$+ \sum_{\boldsymbol{m}\in\mathscr{Y}}\sum_{\boldsymbol{m}'\in\mathscr{Z}}[c(\boldsymbol{n},\boldsymbol{m},\boldsymbol{m}',\boldsymbol{J}) + c(\boldsymbol{n},\boldsymbol{m},-\boldsymbol{m}',\boldsymbol{J})]$$
$$+ \sum_{\boldsymbol{m}\in\mathscr{Z}}\sum_{\boldsymbol{m}'\in\mathscr{Y}}[d(\boldsymbol{n},\boldsymbol{m},\boldsymbol{m}',\boldsymbol{J}) + d(\boldsymbol{n},\boldsymbol{m},-\boldsymbol{m}',\boldsymbol{J})] \tag{35}$$

the Hamiltonian allows for the expression:

$$\mathscr{H}(\boldsymbol{J},\boldsymbol{\varphi}) = H_0(\boldsymbol{J}) + \varepsilon^2 \sum_{\boldsymbol{n}\in\mathscr{A}} \mathbb{D}(\boldsymbol{n},\boldsymbol{J})\cos(\boldsymbol{n}\cdot\boldsymbol{\varphi}). \tag{36}$$

Close to any resonant action associated with a resonant vector at $\mathcal{O}(\varepsilon^2)$, $\boldsymbol{n}$, we could apply the pendulum approximation to get the same formal expression for the resonant Hamiltonian given by (17).

The variations in the energy components are similar to those of $\mathcal{O}(\varepsilon)$; indeed,

$$\Delta h_i = \tfrac{8}{3} A J_i^{1/3} (\mu|\mathscr{U}_0|)^{1/2} n_i.$$

For those $\boldsymbol{n}$ with either $n_3 = 0$ or $n_2 = 0$, the resonant curves are given by Eqs. (25) and (26), respectively, with the pertinent substitution of m_i and I_i by n_i and J_i. Meanwhile, whenever $n_1 = 0$ the resonant curves are given by

$$\begin{cases} J_2^r = \dfrac{1}{(1+(n_2/n_3)^4)^{3/4}}\left\{\dfrac{h}{A} - (J_1^r)^{4/3}\right\}^{3/4}, \\[4mm] J_3^r = \dfrac{1}{(1+(n_3/n_2)^4)^{3/4}}\left\{\dfrac{h}{A} - (J_1^r)^{4/3}\right\}^{3/4} \end{cases} \tag{37}$$

with $J_1^r \in [0,(h/A)^{3/4}]$.

Let $\mathscr{V}_r(\varepsilon^2, 1/23^2)$ be the set of resonant vectors which belong to $\mathscr{A}$ and that can be constructed by at least one pair $(\boldsymbol{m},\boldsymbol{m}')$ such that $\mathcal{O}(\alpha_{\boldsymbol{m}}\alpha_{\boldsymbol{m}'}) \leqslant \mathcal{O}(1/23^2)$. On computing the elements of $\mathscr{V}_r(\varepsilon^2, 1/23^2)$ we learn that this set consists of 15 vectors with one null component together with 48 having all its three components different from zero.

Fig. 7 shows the area of the canonical energy surface ($h = 0.485$) occupied by those resonances at $\mathcal{O}(\varepsilon^2, 1/23^2)$ that have one null com-

ponent together with the $(2,-1,-1)$ resonance, for the same two values of the perturbative parameter used for Fig. 6.

Such a subset of $\mathscr{V}_r(\varepsilon^2, 1/23^2)$ as well as the complete set $\mathscr{V}_r(\varepsilon, 1/23^2)$ have been considered in Fig. 8–left for $\varepsilon = 0.005$. This picture should be compared with the contour–plot obtained by means of the MEGNO for the very same value of ε, which is displayed in Fig. 8–right (taken from [10]). This numerical exploration evinces that the resonances which strongly manifest are those with just one null component (i.e. the straight ones) and the $(2,-1,-1)$ resonance (the one showing a curved shape).

A glance at Fig. 8–left reveals that in some intersections between $\mathcal{O}(\varepsilon)$ and $\mathcal{O}(\varepsilon^2)$ resonances, the widths of the latter tend asymptotically to infinity. This is due to the emergence of small denominators in the Fourier coefficients of the perturbation, a fact that reminds us that the canonical transformation performed in order to eliminate the perturbation terms proportional to ε is no longer valid in the neighbourhood of any $\mathcal{O}(\varepsilon)$ resonance.

A good example of this behaviour is the intersection between the $(0,1,-1)$ and the $(2,-1,0)$ resonances. The former is an $\mathcal{O}(\varepsilon^2)$ resonance that starts on the top right-hand corner of the energy surface and gets through the middle of it while the latter is of $\mathcal{O}(\varepsilon)$ and can be identified as the widest of the resonances departing from the bottom right-hand corner of the energy surface.

10. Analytical estimate of the critical value of the perturbation parameter for the 3D system

As it can be seen from Fig. 8, many resonances have a triangular shape. Such is the case of all those resonances associated with a vector having either its second or its third component equal to zero.

It can be demonstrated instead that for a resonant vector with its first component n_1 equal to zero, the coefficients $a(\boldsymbol{n},\boldsymbol{m},\pm\boldsymbol{m}',\boldsymbol{J})$ and $b(\boldsymbol{n},\boldsymbol{m},\pm\boldsymbol{m}',\boldsymbol{J})$ are null $\forall(\boldsymbol{m},\boldsymbol{m}')$. Thus, the contribution of such a vector proceeds only through its concomitant coefficients $c(\boldsymbol{n},\boldsymbol{m},\pm\boldsymbol{m}',\boldsymbol{J})$ and $d(\boldsymbol{n},\boldsymbol{m},\pm\boldsymbol{m}',\boldsymbol{J})$. Further, from Eq. (37) it can be stated that the resonance width tends to zero when J_1 approaches either 0 or $(h/A)^{3/4}$. Consequently, the regions encompassed by the separatrices of resonances for which $n_1 = 0$ do not have a triangular shape.

On estimating ε_c for the 3D model, we are compelled to make somewhat strong simplifications: (i) we take as ε_c the value of ε for which the total area covered by resonant regions (A_r) equals 90% of the whole area of the energy surface (A_h); (ii) we approximate by triangles the resonant regions corresponding to resonant
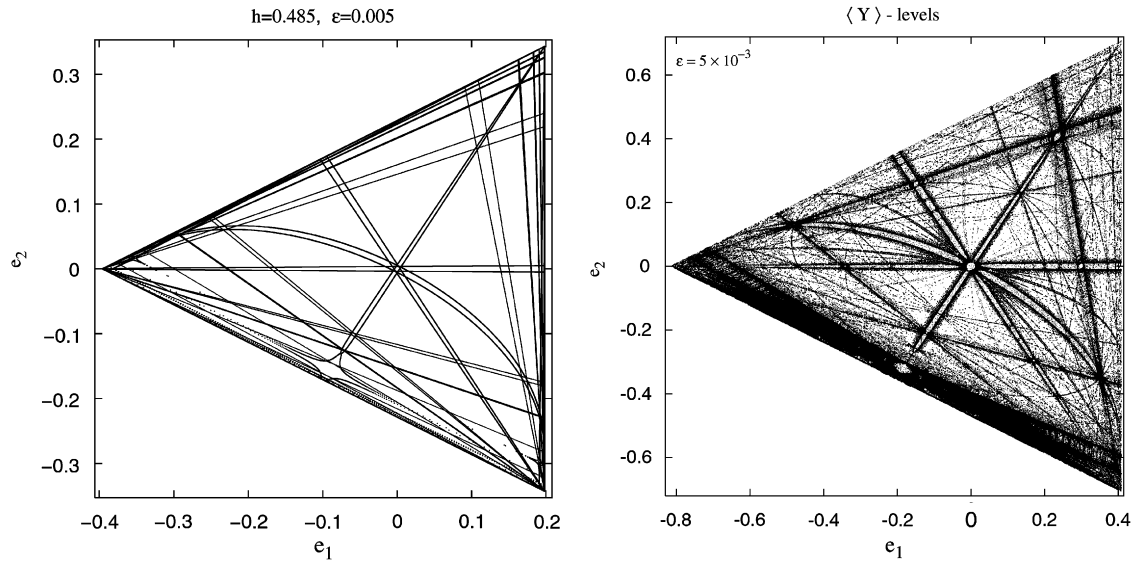
Fig. 8. Resonances up to $\mathcal{O}(\varepsilon^2, 1/23^2)$ for $\varepsilon = 0.005$ (on the left) and the actual resonance structure obtained with the MEGNO (on the right) for the same energy normalized to $h = 1$.
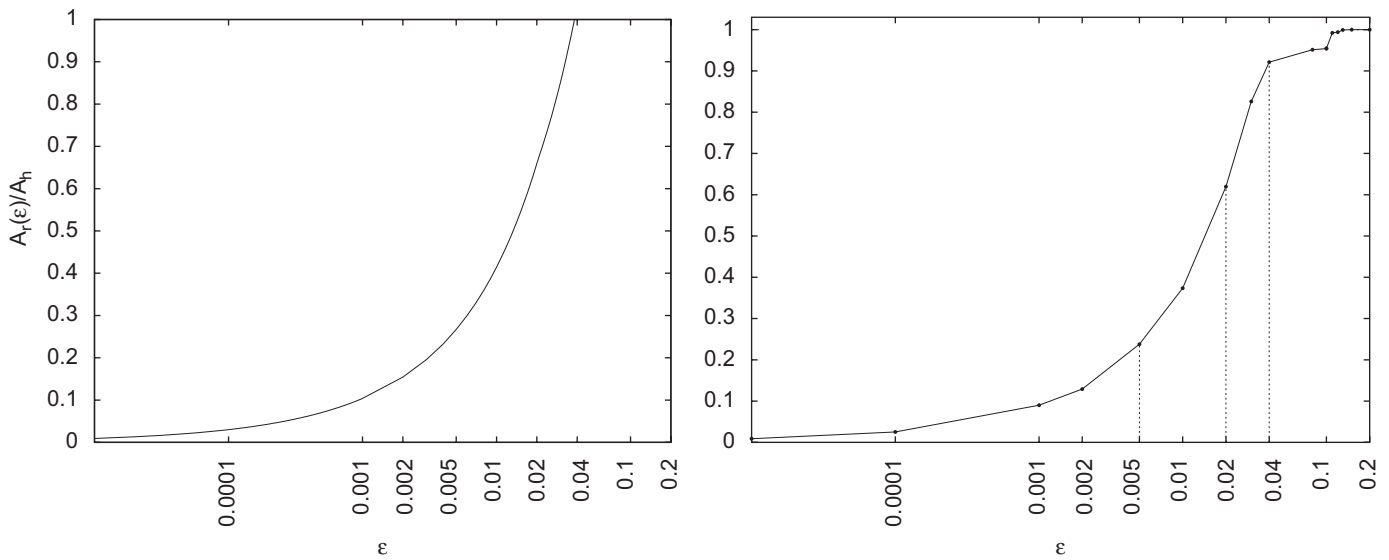

Fig. 9. A_r/A_h (on the left) and fraction of chaotic motion (on the right) both vs. the perturbation parameter, in logarithmic scale.

vectors with one null component; (iii) we approximate by two triangles the resonant region corresponding to the $(2, -1, -1)$ resonance; (iv) we do not consider any further resonance; (v) we add up the area of each resonance disregarding the intersections due to crossings of resonances, so that those regions corresponding to two different resonances are considered twice.

In Fig. 9–left we have plotted the fraction A_r/A_h for the perturbation parameter varying in the range $\varepsilon \in [0.00001, 0.2]$. There it can be observed that $A_r(\varepsilon)$ reaches 90% of A_h for some ε_c between 0.03 and 0.04. This result is in quite good agreement with that arising from Fig. 9–right (taken from [12]) which displays the fraction of chaotic motion according to the MEGNO values, for the same range of ε.

11. Discussion

We have checked out the accuracy of the overlap criterion when applied to a simple near-integrable Hamiltonian system in both its 2D and 3D versions. To this end, we have computed the unperturbed resonances up to order $\mathcal{O}(\varepsilon^2)$ for both systems, and modelled each resonance by means of the pendulum approximation in order to estimate the theoretical critical value of the perturbation parameter for a global transition to chaos.

By performing several SOS for the 2D case we have derived an empirical value to be compared to our theoretical estimation. There is a significant difference between both values which might be due to not having considered the width of the perturbed separatrix layers in the theoretical estimation.

For the 3D case a theoretical estimate of the critical parameter has been attained, which is shown to match the one given in [12], where such a value is achieved on computing the fraction of chaotic motion vs. ε according to the MEGNO values.

Let us remark that the conception of transition to global chaos assumed for the numerical estimate of ε_c in the 2D case is of a different nature from the one adopted for the 3D system. Actually, the 2D

system is considered to be globally chaotic if the chaotic component of phase space appears almost fully connected, while in the 3D case the system is regarded as globally chaotic when at most 10% of the energy surface corresponds to invariant tori. Notice that in the latter case, though it is very likely that the chaotic component be connected when resonances do overlap in a mostly chaotic phase space, nothing could be asserted about the existence of a fully connected region of unstable motion (see [12,14,15] for a thorough discussion).

Therefore, from both theoretical and numerical results we may assert that a suitable estimate for the critical value of the perturbation parameter could be obtained, for the 3D model, by means of the overlap criterion when considering resonances up to $\mathcal{O}(\varepsilon^2)$. Indeed, regarding terms just up to $\mathcal{O}(\varepsilon)$ largely overestimates ε_c, as already shown by [1] for the standard map.

Acknowledgements

References

[1] B.V. Chirikov, A universal instability of many-dimensional oscillator systems, Phys. Rep. 52 (5) (1979) 263–379.
[2] L.E. Reichl, The Transition to Chaos, vols. I and II, Springer, New York, 1992.
[3] A.N. Kolomogorov, On the conservation of conditionally periodic motions for a small change in the Hamiltonian function [in Russian], Dokl. Akad. Nauk SSSR 98 (1954) 527–530.
[4] J.K. Moser, On invariant curves of area-preserving mappings of an annulus, Nachr. Akad. Wiss. Gottingen Math. Phys. Kl. II (1962) 1–20.
[5] V.I. Arnol'd, Proof of A.N. Kolmogorov's theorem on the conservation of conditionally periodic motions with a small variation in the Hamiltonian, Russ. Math. Surv. 18 (1963) 9–36.
[6] A. Giorgilli, New insights on the stability problem from recent results in classical perturbation theory, in: D. Benest, C. Froeschlé (Eds.), Modern Methods in Celestial Mechanics, Editions Frontières, Gif-sur-Yvette, 1990, pp. 249–284.
[7] J. Wisdom, The resonance overlap criterion and the onset of stochastic behavior in the restricted three-body problem, Astron. J. 85 (1980) 1122–1133.
[8] J.J. Lissauer, Urey prize lecture: on the diversity of plausible planetary systems, Icarus 114 (1995) 217–236.
[9] L.R. Mudryk, Y. Wu, Resonance overlap is responsible for ejecting planets in binary systems, Astrophys. J. 639 (2006) 423–431.
[10] P.M. Cincotta, C.M. Giordano, C. Simó, Phase space structure of multidimensional systems by means of the mean exponential growth factor of nearby orbits, Physica D 182 (2003) 151–178.
[11] I.S. Gradshteyn, I.M. Ryzhik, Table of Integrals, Series and Products, Academic Press, New York, 1980.
[12] C.M. Giordano, P.M. Cincotta, Chaotic diffusion of orbits in systems with divided phase space, Astron. Astrophys. 423 (2004) 745–753.
[13] P.M. Cincotta, Arnold diffusion: an overview through dynamical astronomy, NewAR 46 (2002) 13–39.
[14] P.M. Cincotta, C.M. Giordano, M.J. Pérez, Global dynamics in galactic triaxial systems I, Astron. Astrophys. 455 (2006) 499–507.
[15] P.M. Cincotta, C.M. Giordano, Topics on diffusion in phase space of multidimensional Hamiltonian systems, in: T.B. Perlidze (Ed.), New Nonlinear Phenomena Research, Nova Science Publishers, Hauppauge, NY, 2008, pp. 393–410.